Preprints of the 18th IFAC World Congress
Milano (Italy) August 28 - September 2, 2011

# A modular approach to dynamic modelling of heat exchangers in vapor compression cycles

**Andrea Tilli** * **Roberto Diversi** *

* *CASY-DEIS - Department of Electronics, Computer Science and Systems, University of Bologna, Viale del Risorgimento 2, 40136 Bologna, Italy (e-mail: andrea.tilli@unibo.it, roberto.diversi@unibo.it).*

**Abstract:** This paper describes a modular approach to the dynamic modelling of heat exchangers (condenser and evaporator) in vapor compression cycles. The model of the heat exchangers is obtained by properly connecting a small number of generic modules where a fluid flows, exchanging heat and, possibly, changing state (from liquid to vapor and vice-versa). The dynamic model of the generic element is phase–independent and is valid in every working condition. Unlike other approaches described in the literature, the mass exchange rate from vapor to liquid is explicitly computed in order to comply with state-trajectories constraints which are defined according to the current phase condition and highlighting when a phase-transition is possible. This leads to an effective representation of constrained evolutions and smooth jumps among different phases. The proposed dynamic elements are characterized by dynamic-orientation of some interface variables; this crucial feature for correct modelling is treated carefully in composing them and a suitable standardized interface is defined.

Keywords: Dynamic modelling, heat exchangers, vapor compression cycles, refrigerators, two–phase flow.

## 1. INTRODUCTION

The most important method of converting work to move energy from one spatial location to another is the vapor compression cycle (VCC). It is widely used in domestic and commercial refrigeration systems and in heating, ventilating and air conditioning (HVAC) systems. A proper control and diagnosis of VCC systems is of great importance in order to improve both energy efficiency and machine reliability. These tasks need suitable dynamic models that should be characterized by a good trade-off between accuracy and complexity.

The basic scheme adopted in VCC systems is composed by four major components (see Fig. 1): a compressor, a condenser, an expansion valve and an evaporator. Due to the different time constants involved, the dynamics of compressor and expansion valve can be assumed as much faster than those of condenser and evaporator. Hence, compressor and expansion valve are usually considered as static components and the dynamic of the whole cycle is fully governed by the heat exchangers. The dynamical modelling of heat exchangers has thus receveid an increasing attention in the literature, see (Bendapudi and Braun, 2002; Alleyne et al., 2007) and the references therein.

Modelling the dynamic behavior of heat exchangers is a challenging task since physical state transitions of the fluid usually take place in such components. During normal operating conditions both the condenser and evaporator are characterized by different and dynamically-varying regions, each of which shows different phase conditions, namely *superheated* (only vapor is present), *saturated* (a two–phase state where vapor and liquid can coexist permanently) and *subcooled* (only liquid is present). It is worth to stress that, on the one hand, the phase condition arising in a region depends on the evolution of the thermodynamics state variables (such as temperature and pressure) and, on the other hand, when a particular phase condition is reached, it can determine some constraints on the evolutions of the above mentioned state variables. A suitable dynamic model should thus be sufficiently accurate to capture these crucial aspects but of relatively low complexity for control design purposes. Distributed–parameter models, that could be the more natural choice when dealing with thermo-fluid systems do not satisfy this trade-off hence, accurate lumped–parameter models are required.

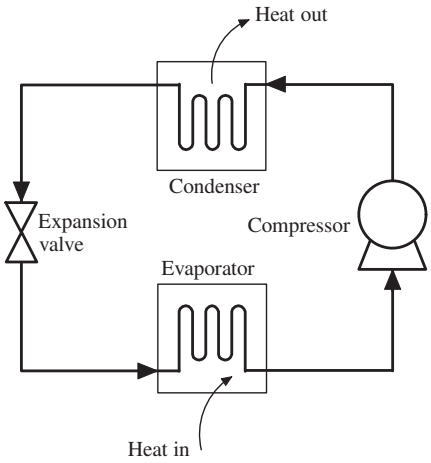



Fig. 1. Schematic diagram of a vapor compression cycle.

With reference to lumped–parameter models, two main modelling techniques can be considered: finite difference methods and moving boundary methods. In the finite difference approach, the governing conservation equations are approximated by a finite difference scheme that consists in dividing the heat exchangers into a number of elements, each of which charac-

Copyright by the
International Federation of Automatic Control (IFAC)

terized by its own state properties (Gruhle and Isermann, 1985; MacArthur and Grald, 1989). This approach leads to phase–independent models whose accuracy increases with the number of elements. However, since the complexity increases with the number of elements as well, the obtained models are, in general, computationally very expensive.

The moving boundary approach consists in dividing the heat exchangers into sections (in general two or three) of variable volume according to the state of the refrigerant, i.e. saturated, superheated, subcooled (He et al., 1997; Willatzen et al., 1998; Leducq et al., 2003; Zhang and Zhang, 2006; McKinley and Alleyne, 2008). In order to capture the essential of the two–phase flow dynamics it is important to track the boundaries between adjacent zones so that some zone lengths are chosen as state variables. This method is phase–dependent but leads to dynamic models of fairly low order. Special attention needs to be given to the large scale transients, caused by load changes, start-up, shutdown and feedback control (Bendapudi and Braun, 2002). In fact, in such situations, both the creation and disappearence of two–phase, superheated and subcooled zones must be properly taken into account. This problem has been treated only in few papers (Pettit et al., 1998; Zhang and Zhang, 2006; McKinley and Alleyne, 2008; Bin and Alleyne, 2009).

Starting from the work described in (Tilli and Diversi, 2010), the aim of this paper is to develop a phase–independent dynamic model of fairly low order for a generic heat exchanger, which is valid in every working condition i.e.in both small and large transients. A modular approach is exploited. The whole model is obtained by properly connecting a small number (two or three) of phase–independent generic modules where the fluid flows, exchanging heat and, possibly, changing state (from liquid to vapor and vice-versa). Each element is characterized by a single temperature state and pressure state. Fluid phase-transition and evolution constraints in subcooled, saturated and superheated phases are directly taken into account, preserving mass and energy balances. The mass exchange rate from vapor to liquid is explicitly computed in order to comply with state-trajectories constraints, which are defined according to the current phase condition and highlighting when a phase-transition is possible. Constrained evolutions and smooth jumps among different phases are thus represented effectively without using switching state variables. In order to achieve a correct modelling of the heat exchanger behavior, the orientation of some interface variables among adjacent elements vary according to the dynamic evolution. This issue has been carefully addressed, defining a standardized interface which leads to effectively composable dynamically-oriented modules.

The organization of the paper is as follows. In Section 2 the model underlying each single element is described, also recalling (Tilli and Diversi, 2010). The mechanism adopted to handle transitions and constraints related to different phase–states is carefully described, together with the interface variables. In Section 3, the composition of different modules is described. Resistive elements for suitable coupling are introduced. Particular attention is payed to the implementation of dynamic-orientation mechanism in MATLAB/SIMULINK$^{TM}$ framework. Finally, in Section 4 simulations results are presented and discussed referring to a simple, yet significative, example.

Table 1. Nomenclature

| Variables: | | Subscripts: | |
|---|---|---|---|
| $J_Q$ | heat transfer rate | $AUX$ | auxiliary |
| $P$ | pressure | $I$ | inlet |
| $S$ | section | $L$ | liquid |
| $T$ | temperature | $O$ | outlet |
| $V$ | volume | $T$ | total (liquid + vapor) |
| $h$ | specific enthalpy | $V$ | vapor |
| $\ell$ | length | $W$ | wall |
| $q$ | volumetric flow | | |
| $u$ | specific internal energy | | |
| $x$ | vapor quality | | |
| $\rho$ | density | | |
| $\omega$ | mass flow | | |

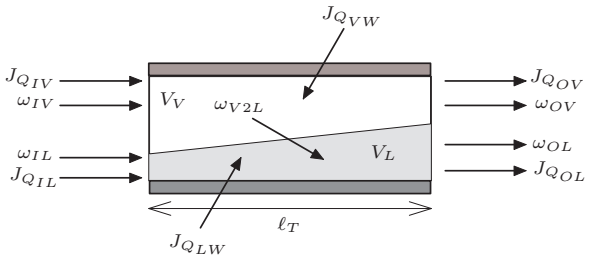



Fig. 2. The generic element when saturated conditions occur.

## 2. DYNAMIC MODEL OF A GENERIC ELEMENT

The generic element under consideration consists in a fixed space volume completely filled by fluid where the fluid flows exchanging heat with the environment, possibly changing its physical state. The following assumptions will be considered as satisfied:

- The refrigerant flow is one-dimensional.
- The element has a cylindrical shape with open basis and closed lateral surface. It follows that mass and energy can be exchanged through the basis while only heat can be exchanged through the lateral surface.
- Both temperature and pressure are uniform within the volume.
- Kinetic energy of the refrigerant is assumed as negligible, hence the momentum equation is not considered even when multiple modules are connected.

In the sequel, one of the two basis will be referred as inlet port, while the other as outlet port. The adopted nomenclature is reported in Table 1. The total mass flow at input port $\omega_{IT}$ is considered as "positive" when incoming while the total mass flow at output port, $\omega_{OT}$ is "positive" when outgoing. The total heat transfer rate through the element wall (lateral surface), $J_{Q_W}$ is "positive" when incoming.

As already said, the physical state of the fluid in not a priori fixed and it will depend on the dynamic evolution. The model is thus phase–independent. Three possible phase conditions can occur: *superheated*, a single–phase state where only vapor is present; *saturated*, a two–phase state where vapor and liquid can coexist permanently; *subcooled*, a single–phase state where only liquid is present. Fig. 2 refers to the saturated condition.

To obtain a state space model, mass and energy balances for vapor and liquid are considered:

$$\frac{\partial \rho_L}{\partial P} V_L \dot{P} + \frac{\partial \rho_L}{\partial T} V_L \dot{T} + \rho_L \dot{V}_L = \omega_{IL} - \omega_{OL} + \omega_{V2L} \quad (1)$$

$$\frac{\partial \rho_V}{\partial P} V_V \dot{P} + \frac{\partial \rho_V}{\partial T} V_V \dot{T} + \rho_V \dot{V}_V = \omega_{IV} - \omega_{OV} - \omega_{V2L} \quad (2)$$

$$\rho_L V_L \dot{u}_L(T) + u_L(T)(\omega_{IL} - \omega_{OL}) = +h_{IL}\omega_{IL} + - h_{OL}\omega_{OL} - u_L(T)\omega_{V2L} + J_{Q_{LW}} + J_{Q_{IL}} - J_{Q_{OL}} \quad (3)$$

$$\rho_V V_V \dot{u}_V(T) + u_V(T)(\omega_{IV} - \omega_{OV}) = +h_{IV}\omega_{IV} + - h_{OV}\omega_{OV} + u_V(T)\omega_{V2L} + J_{Q_{VW}} + J_{Q_{IV}} - J_{Q_{OV}} \quad (4)$$

where $\omega_{V2L}$ represents the vapor-to-liquid conversion ratio occurring in the observed volume and $\omega_{IV} = x_I\omega_{IT}$, $\omega_{IL} = (1 - x_I)\omega_{IT}$, $\omega_{OV} = x_O\omega_{OT}$, $\omega_{OL} = (1 - x_O)\omega_{OT}$. No heat exchange occurs between liquid and vapor in the element since the temperature is assumed as uniform. It is also necessary to known the consitutive equations $\rho_L = \rho_L(P, T)$, $\rho_V = \rho_V(P, T)$ and the functions $u_L = u_L(T)$, $u_V = u_V(T)$, together with their partial derivatives w.r.t. $P$ and/or $T$. These functions can be found in literature for a specific fluid (Lemmon et al., 2008).

*Remark 1.* In the two–phase (saturated) condition $u_V(\bar{T}) \geq u_L(\bar{T})$, $\forall \bar{T}$ and the difference $u_V(\bar{T}) - u_L(\bar{T})$ represents the so called *specific latent heat* stored in (released from) the internal energy of each mass unity when a liquid-to-vapor (vapor-to-liquid) transition occurs.

*Remark 2.* No dependence on $P$ is considered for the internal energies $u_L$ and $u_V$; this is admissible since their actual relation with pressure is negligible for most of the fluids used in VCC. This assumption can however be easily removed if necessary.

Pressure, temperature and liquid volume are chosen as state variables; the inputs are the total mass flows at inlet and outlet ports and the heat transfer rate trough the element wall (lateral surface). By suitably handling equations (1)–(4) and taking into account that $V_T = V_V + V_L$ and $\dot{V}_T = 0$ it is possibile to obtain a state space model of type (see (Tilli and Diversi, 2010) for further details)

$$\begin{bmatrix} \dot{T} \\ \dot{P} \\ \dot{V}_L \end{bmatrix} = \begin{bmatrix} f_T(T, P, V_L, \omega_{IL}, \omega_{IV}, \omega_{OL}, \omega_{OV}, \omega_{V2L}) \\ f_P(T, P, V_L, \omega_{IL}, \omega_{IV}, \omega_{OL}, \omega_{OV}, \omega_{V2L}) \\ f_{V_L}(T, P, V_L, \omega_{IL}, \omega_{IV}, \omega_{OL}, \omega_{OV}, \omega_{V2L}) \end{bmatrix} = \begin{bmatrix} f_{T_1}(\cdot) + f_{T_2}(\cdot)\,\omega_{V2L} \\ f_{P_1}(\cdot) + f_{P_2}(\cdot)\,\omega_{V2L} \\ f_{V_{L1}}(\cdot) + f_{V_{L2}}(\cdot)\,\omega_{V2L} \end{bmatrix}. \quad (5)$$

A crucial issue of the proposed modelling approach concerns the explicit computation of the mass exchange rate $\omega_{V2L}$ between vapor and liquid. In fact, $\omega_{V2L}$ needs to be carefully defined to comply with the constraints on model evolutions related to the particular phase condition. These constraints can be described by considering a pressure–temperature diagram (see Fig. 3). In the $P$-$T$ diagram, it is possible to identify two regions separated by a curve, i.e. by the saturation curve, that will be represented by the relation

$$c_{SAT}(T, P) = T - T_{SAT}(P) = 0. \quad (6)$$

The computation of $\omega_{V2L}$ is based on the following rules.

- In the low-pressure and high-temperature region superheated phase takes place (i.e. $c_{SAT}(T, P) > 0$ or, equivalently, $T > T_{SAT}(P)$), hence the liquid volume and its derivative have to be identically null ($V_L = \dot{V}_L = 0$). As a consequence, $\omega_{V2L}$ must be null as well.
- In the high-pressure low-temperature region subcooled phase occurs (i.e. $c_{SAT}(T, P) < 0$ or, equivalently, $T < T_{SAT}(P)$) so that the liquid volume must equal the total volume ($V_L = V_T$). Again, $\omega_{V2L}$ has to be null.
- On the saturation curve saturated phase takes place (i.e. $c_{SAT}(T, P) = 0$) and the liquid volume can evolve assuming values in the interval between zero and the total volume value ($V_L \in ]0,\ V_T[$). $\omega_{V2L}$ has to be computed to guarantee sliding on saturation curve i.e. $[f_T(\cdot),\ f_P(\cdot)] \cdot \left[1,\ -\frac{dT_{SAT}(P)}{dP}\right]^T = 0$, since the permanent coexistence of vapor and liquid is possible on the saturation curve only (see the upper part of Fig. 3).
- No direct jump from subcooled region to superheated one, or vice-versa, is allowed so that when the state trajectories approach the saturation curve with a vector $[f_{P_1}\ f_{T_1}]^T$ directed toward the opposite phase region (from superheated towards subcooled or vice-versa) pressure and temperature are constrained in evolving along the curve. $\omega_{V2L}$ has thus to be computed in order to obtain a state trajectory sliding on the saturation curve, i.e. $[f_T(\cdot),\ f_P(\cdot)] \cdot \left[1,\ -\frac{dT_{SAT}(P)}{dP}\right]^T = 0$, (see the upper part of Fig. 3 again), while $V_L$ is changing accordingly.
- When the current state belongs to the saturation curve, but $V_L = 0$ or $V_L = V_T$ and the vector $[f_{P_1}\ f_{T_1}]^T$ is directed to the superheated zone in the former case, while is directed toward the subcooled zone in the latter, $\omega_{V2L}$ is set to zero and the state trajectory can leave the saturation curve (see the lower part of Fig. 3).

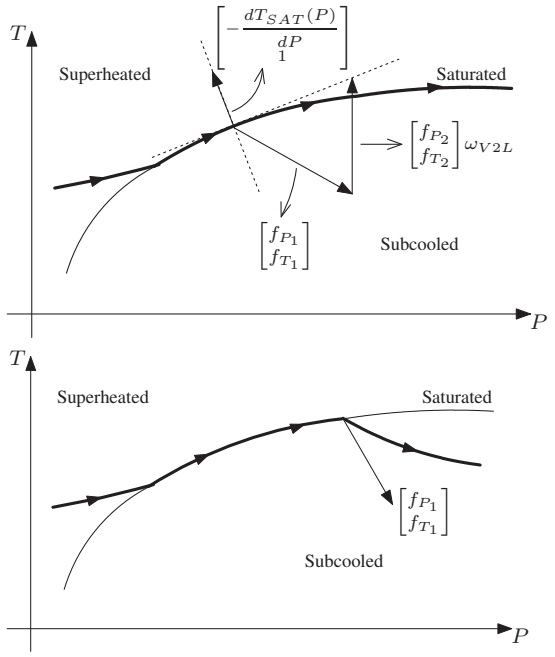



Fig. 3. Examples of constrained evolutions on the $P$-$T$ plane

The extended mathematical version of the above rules is reported in (10), where some additional marginal cases are considered, see (Tilli and Diversi, 2010).

To complete the model, the vapor quality and the specific entalphies at inlet and outlet ports are computed according to Table 2, whose rationale is the following.

- When the total mass flow at an $I/O$ port is incoming, both the vapor quality and the specific enthalpies are fixed by the outside so that they are considered as auxiliary inputs (denoted by the suffix $AUX$).
- When the total mass flow at an $I/O$ port is outgoing, the specific enthalpies for liquid and vapor can be straightforwardly derived from $T$ and $P$ of the observed volume; the vapor quality is derived from the volume behavior, too, but according to the functions $f(\cdot)$, $f_O^I(\cdot)$, $f_I^O(\cdot)$ which are defined according to the following rules:
  - If a single-phase condition (i.e. subcooled or superheated) takes place in the observed volume, the vapor title at the ports where the flow is outgoing is null, for subcooled condition, or equal to one, for superheated condition.
  - If the volume is in two-phase condition (i.e. saturated) a more sophisticated strategy is adopted. First, a linear distribution of liquid and vapor volumes over the total volume is assumed, i.e. the surface occupied by liquid and vapor at each section (usually represented by the so-called *void fraction*) is linearly varying along $\ell_T$. Moreover, homogeneous fluid flow is assumed, i.e. the vapor and liquid speeds are equal (Rice, 1987). It follows that the surface occupied by liquid/vapor at input/output port is proportional to the liquid/vapor-to-total volumetric flow ratio. Hence if a volumetric flow ratio is fixed by outside at one port, while the other one is depending on the volume dynamics, then the latter can be computed according to the previous considerations as reported in (7), (8) and (9). When both the input and output flows are outgoing or null, the volumetric distribution is assumed uniform along $\ell_T$ and the vapor title is fixed accordingly.

The resulting equations are reported below

$$f\left(V_L,\, \rho_L,\, \rho_V\right) = \left(1 + \frac{\rho_L}{\rho_V}\frac{V_L}{V_T - V_L}\right)^{-1} \tag{7}$$

$$f_I^O\left(V_L,\, x_I,\ \rho_L,\, \rho_V\right) = \begin{cases} 0 & \text{if } \ell_V \le \ell \\ \left(1 + \dfrac{\rho_L}{\rho_V}\dfrac{S_T - S_V}{S_V}\right)^{-1} & \text{if } \ell_V > \ell \text{ and } S_V < S_T \\ 1 & \text{if } \ell_V > \ell \text{ and } S_V \ge S_T \end{cases} \tag{8}$$

where

$$\ell_V = 2\frac{V_T - V_L}{S_T}\frac{q_{IT}}{q_{IV}}, \quad S_V = 2\frac{V_T - V_L}{\ell} - S_T\frac{q_{IV}}{q_{IT}}, \quad \frac{q_{IV}}{q_{IT}} = \left(1 + \frac{\rho_V}{\rho_L}\left(\frac{1}{x_I} - 1\right)\right)^{-1}$$

$$f_O^I\left(V_L,\, x_O,\ \rho_L,\, \rho_V\right) = \begin{cases} 0 & \text{if } \ell_V \le \ell \\ \left(1 + \dfrac{\rho_L}{\rho_V}\dfrac{S_T - S_V}{S_V}\right)^{-1} & \text{if } \ell_V > \ell \text{ and } S_V < S_T \\ 1 & \text{if } \ell_V > \ell \text{ and } S_V \ge S_T \end{cases} \tag{9}$$

where

$$\ell_V = 2\frac{V_T - V_L}{S_T}\frac{q_{OT}}{q_{OV}}, \quad S_V = 2\frac{V_T - V_L}{\ell} - S_T\frac{q_{OV}}{q_{OT}}, \quad \frac{q_{OV}}{q_{OT}} = \left(1 + \frac{\rho_V}{\rho_L}\left(\frac{1}{x_O} - 1\right)\right)^{-1}$$

*Remark 3.* It is worth to note that the input/output variables of the generic module are not a priori fixed but can be dynamically varying. The developed dynamic model can thus be considered as a non oriented model. This aspect must be properly taken into account when more elements are connected to obtain the mathematical models of the whole heat exchangers.

## 3. COMPOSITION OF GENERIC ELEMENTS

In Fig. 4 the general structure of the composition of the proposed dynamical elements is reported. Mass and heat conduction flow between two adjacent element is computed inserting resistive elements.
Often heat conduction along the fluid and the wall sections from a module to another is considered negligible with respect to the energy transferred by mass flow. Nevertheless, in this approach it is considered, since it is straightforward and it allows to obtain a better modelling when small mass flow occurs.
As far as the mass flow is concerned, it is worth noting that interface pressure drops will generate an energy conversion from mechanic power to thermal power. This phenomenon does not require additional terms in the balances since, according to the proposed interface, the enthalpy incoming in a port is exactly the one outgoing from the adjacent. The fluidic resistive element, adopted for connection, will change the amount of mechanical and thermal power composing the transferred enthalpy, but not its total value.
According to Section 2, the vapor title $x$, vapor and liquid enthalpies, $h_V$ and $h_L$ at inlet and outlet ports of each element will be defined by the considered element or by the adjacent ones according to the direction of the interface mass flow. Hence these variables have an input or an output role depending on the dynamic evolution of the system. In order to reproduce this behavior in strictly-oriented Matlab/Simulink framework, avoiding the so-called *algebraic loops*, additional variables $x_{I/Ob}$, $h_{I/OVb}$ and $h_{I/OLb}$ have been added at the interface to be connected to the corresponding $AUX$ variables of the adjacent element. Values of such variables are reported in Table 3.

## 4. SIMULATIONS AND DISCUSSION

In this Section the effectiveness of the proposed modelling approach is discussed considering simulations results in two simple, yet very significant, cases. In both cases, two elements, namely *Module 1* and *Module 2* are cascade connected. Each module has a reference volume with $S_T = 154\text{mm}^2$ and $\ell_T = 0.5\text{m}$. R134a is the adopted fluid (see (Lemmon et al., 2008) for all the characteristics). A thermal conduction resistance of $R_{TH} = 16°\text{C/W}$ is assumed between the outlet port of Module 1 and the inlet one of Module 2, for both of the considered tests. Differently, for the fluidic resistance between the same port two different values are assumed in the two tests, $R_{fluid} = 0.3\text{MPa/(kg/s)}$, in the first test, $R_{fluid} = 3\text{MPa/(kg/s)}$, in the second one.
In both tests, the outlet port of Module 2 is closed and the same vapor flow is imposed at the inlet port of Module 1. In

$$\omega_{V2L} = \begin{cases} \bar{\omega}_{V2L} \text{ s.t. } f_{V_L}(\cdot) = 0 & \text{if} \quad c_{SAT}(T,\, P) \neq 0 \\ & \text{or} \left[ c_{SAT}(T,\, P) = 0 \text{ and } V_L = 0, \text{ and } (\omega_{IL} - \omega_{OL}) > 0 \text{ and} \right. \\ & \quad \left( \bar{\omega}_{V2L} < -(\omega_{IL} - \omega_{OL}), \right. \\ & \quad \left. \left. \text{where } \bar{\omega}_{V2L} \text{ s.t. } [f_T(\cdot),\, f_P(\cdot)] \cdot \left[1,\, -\frac{dT_{SAT}(P)}{dP}\right]^T = 0 \right) \right] \\ & \text{or} \left[ c_{SAT}(T,\, P) = 0 \text{ and } V_L = V_T, \text{ and } (\omega_{IV} - \omega_{OV}) > 0 \text{ and} \right. \\ & \quad \left( \bar{\omega}_{V2L} > (\omega_{IV} - \omega_{OV}), \right. \\ & \quad \left. \left. \text{where } \bar{\omega}_{V2L} \text{ s.t. } [f_T(\cdot),\, f_P(\cdot)] \cdot \left[1,\, -\frac{dT_{SAT}(P)}{dP}\right]^T = 0 \right) \right] \\ 0 & \text{if} \left[ c_{SAT}(T,\, P) = 0 \text{ and } V_L = 0, \text{ and } \omega_{IL} = 0 \text{ and } \omega_{OL} = 0 \right. \\ & \quad \left. \text{and } [f_T(\cdot),\, f_P(\cdot)]_{\omega_{V2L}=0} \cdot \left[1,\, -\frac{dT_{SAT}(P)}{dP}\right]^T \geq 0 \right] \\ & \text{or} \left[ c_{SAT}(T,\, P) = 0 \text{ and } V_L = V_T, \text{ and } \omega_{IV} = 0 \text{ and } \omega_{OV} = 0 \right. \\ & \quad \left. \text{and } [f_T(\cdot),\, f_P(\cdot)]_{\omega_{V2L}=0} \cdot \left[1,\, -\frac{dT_{SAT}(P)}{dP}\right]^T \leq 0 \right] \\ \bar{\omega}_{V2L} \text{ s.t. } [f_T(\cdot),\, f_P(\cdot)] \cdot \left[1,\, -\frac{dT_{SAT}(P)}{dP}\right]^T = 0 & \text{if} \left[ c_{SAT}(T,\, P) = 0 \text{ and } V_L \in\, ]\, 0,\, V_T\, [ \right] \\ & \text{or} \left[ c_{SAT}(T,\, P) = 0 \text{ and } V_L = 0, \right. \\ & \quad \left. \text{and} \left( [f_T(\cdot),\, f_P(\cdot)]_{\omega_{V2L}=0} \cdot \left[1,\, -\frac{dT_{SAT}(P)}{dP}\right]^T < 0 \right) \right] \\ & \text{or} \left[ c_{SAT}(T,\, P) = 0 \text{ and } V_L = V_T, \right. \\ & \quad \left. \text{and} \left( [f_T(\cdot),\, f_P(\cdot)]_{\omega_{V2L}=0} \cdot \left[1,\, -\frac{dT_{SAT}(P)}{dP}\right]^T > 0 \right) \right] \\ & \text{or} \left[ c_{SAT}(T,\, P) = 0 \text{ and } V_L = 0, \text{ and } (\omega_{IL} - \omega_{OL}) > 0 \text{ and} \right. \\ & \quad \left( \bar{\omega}_{V2L} \geq -(\omega_{IL} - \omega_{OL}), \right. \\ & \quad \left. \left. \text{where } \bar{\omega}_{V2L} \text{ s.t. } [f_T(\cdot),\, f_P(\cdot)] \cdot \left[1,\, -\frac{dT_{SAT}(P)}{dP}\right]^T = 0 \right) \right] \\ & \text{or} \left[ c_{SAT}(T,\, P) = 0 \text{ and } V_L = V_T, \text{ and } (\omega_{IV} - \omega_{OV}) > 0 \text{ and} \right. \\ & \quad \left( \bar{\omega}_{V2L} \leq (\omega_{IV} - \omega_{OV}), \right. \\ & \quad \left. \left. \text{where } \bar{\omega}_{V2L} \text{ s.t. } [f_T(\cdot),\, f_P(\cdot)] \cdot \left[1,\, -\frac{dT_{SAT}(P)}{dP}\right]^T = 0 \right) \right] \end{cases} \tag{10}$$

Table 2. Expressions of vapor quality and specific enthalpies at inlet and outlet ports.

| | $\omega_{IT} > 0$ AND $\omega_{OT} < 0$ | $\omega_{IT} > 0$ AND $\omega_{OT} \geq 0$ | $\omega_{IT} \leq 0$ AND $\omega_{OT} < 0$ | $\omega_{IT} \leq 0$ AND $\omega_{OT} \geq 0$ |
|---|---|---|---|---|
| $x_I$ | $x_{I_{AUX}}$ | $x_{I_{AUX}}$ | $f_O^I(V_L,\, x_O,\, \rho_L,\, \rho_V)$ | $f(V_L,\, \rho_L,\, \rho_V)$ |
| $h_{IL}$ | $h_{IL_{AUX}}$ | $h_{IL_{AUX}}$ | $u_L(T) + \dfrac{P}{\rho_L}$ | $u_L(T) + \dfrac{P}{\rho_L}$ |
| $h_{IV}$ | $h_{IV_{AUX}}$ | $h_{IV_{AUX}}$ | $u_V(T) + \dfrac{P}{\rho_V}$ | $u_V(T) + \dfrac{P}{\rho_V}$ |
| $x_O$ | $x_{O_{AUX}}$ | $f_I^O(V_L,\, x_I,\, \rho_L,\, \rho_V)$ | $x_{O_{AUX}}$ | $f(V_L,\, \rho_L,\, \rho_V)$ |
| $h_{OL}$ | $h_{OL_{AUX}}$ | $u_L(T) + \dfrac{P}{\rho_L}$ | $h_{OL_{AUX}}$ | $u_L(T) + \dfrac{P}{\rho_L}$ |
| $h_{OV}$ | $h_{OV_{AUX}}$ | $u_V(T) + \dfrac{P}{\rho_V}$ | $h_{OV_{AUX}}$ | $u_V(T) + \dfrac{P}{\rho_V}$ |

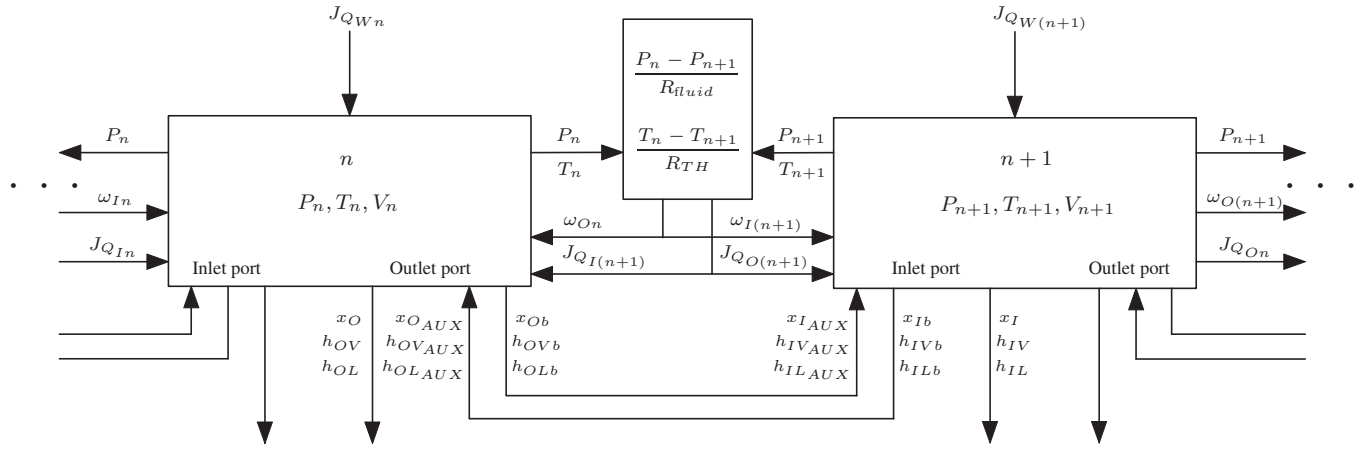



Fig. 4. General scheme for composition of dynamic elements

Table 3. Expressions of additional variables at inlet and outlet ports adopted for dynamic orientation.

| | $\omega_{IT} > 0$ AND $\omega_{OT} < 0$ | $\omega_{IT} > 0$ AND $\omega_{OT} \geq 0$ | $\omega_{IT} \leq 0$ AND $\omega_{OT} < 0$ | $\omega_{IT} \leq 0$ AND $\omega_{OT} \geq 0$ |
|---|---|---|---|---|
| $x_{Ib}$ | $f_O^I(V_L, x_O, \rho_L, \rho_V)$ | $f(V_L, \rho_L, \rho_V)$ | $f_O^I(V_L, x_O, \rho_L, \rho_V)$ | $f(V_L, \rho_L, \rho_V)$ |
| $h_{ILb}$ | $u_L(T) + \frac{P}{\rho_L}$ | $u_L(T) + \frac{P}{\rho_L}$ | $u_L(T) + \frac{P}{\rho_L}$ | $u_L(T) + \frac{P}{\rho_L}$ |
| $h_{IVb}$ | $u_V(T) + \frac{P}{\rho_V}$ | $u_V(T) + \frac{P}{\rho_V}$ | $u_V(T) + \frac{P}{\rho_V}$ | $u_V(T) + \frac{P}{\rho_V}$ |
| $x_{Ob}$ | $f_I^O(V_L, x_I, \rho_L, \rho_V)$ | $f_I^O(V_L, x_I, \rho_L, \rho_V)$ | $f(V_L, \rho_L, \rho_V)$ | $f(V_L, \rho_L, \rho_V)$ |
| $h_{OLb}$ | $u_L(T) + \frac{P}{\rho_L}$ | $u_L(T) + \frac{P}{\rho_L}$ | $u_L(T) + \frac{P}{\rho_L}$ | $u_L(T) + \frac{P}{\rho_L}$ |
| $h_{OVb}$ | $u_V(T) + \frac{P}{\rho_V}$ | $u_V(T) + \frac{P}{\rho_V}$ | $u_V(T) + \frac{P}{\rho_V}$ | $u_V(T) + \frac{P}{\rho_V}$ |

particular, a small vapor input flow, 5g/s, is imposed up to 0.5s, then a step of about 0.5kg/s is applied. A wall thermal resistance $R_{THW}$ equal to 1°C/W is assumed for each module and the external temperature is fixed at 25°C, to determine $J_{Q_W}$ for each module. The initial conditions are $T(0) = 25$°C, $P(0) = 0.1$MPa and $V_L(0) = 0$ for both modules in both tests; in such situation superheated phase takes place.
It is worth noting that some of the above parameters have been set quite different from common parameters of heat exchangers (e.g. both values of $R_{fluid}$ are quite large) in order to make more clear the phenomena in simulations.

The results of the first test, namely Test 1, with small fluidic resistance between modules, i.e. $R_{fluid} = 0.3$MPa/(kg/s), are reported in Figs. 5–11. From Figs. 7 and 8, it can be noted that saturation phase takes place in both modules almost immediately after the step in the input mass flow is applied. Hence vapor to liquid conversion starts rapidly in both modules. At around 0.7s in Module 2 the subcooled phase is reached ($T_2$ in Fig. 8 is lower than $T_{SAT}(P_2)$). Even if pressure and temperature are not so different in the two modules, such behavior, with Module 2 reaching subcooled phase in advance w.r.t. Module 1, is admissible since the incoming mass flow of Module 1 is quickly transferred to the Module 2 (see Figs. 5 and 6) with a low vapor title (see first picture in Fig.11), i.e. with a large amount of liquid. It is worth noting that when subcooled phase occurs in Module 2, the mass flow from Module 1 to 2 immediately falls, according to the increasing of $P_2$ which is related to the lower fluidic capacity of liquid w.r.t. to vapor or vapor-liquid mixtures.

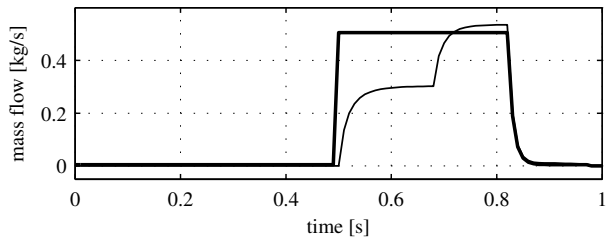



Fig. 5. Test 1: input vapor flow $\omega_{IV1}$ (bold line) and vapor-to-liquid exchange ratio in Module 1 $\omega_{V2L1}$ (thin line).

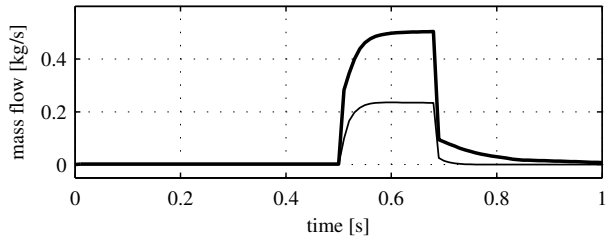



Fig. 6. Test 1: mass flow from Module 1 to Module 2 $\omega_{O1} = \omega_{I2}$ (bold line) and vapor-to-liquid exchange ratio in Module 2 $\omega_{V2L2}$ (thin line).

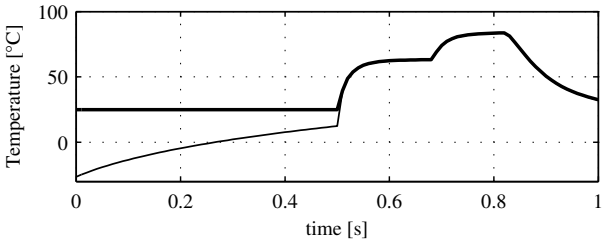



Fig. 7. Test 1: Module 1 temperature $T_1$ (bold line) and saturation temperature corresponding to the current pressure $P_1$ (thin line)

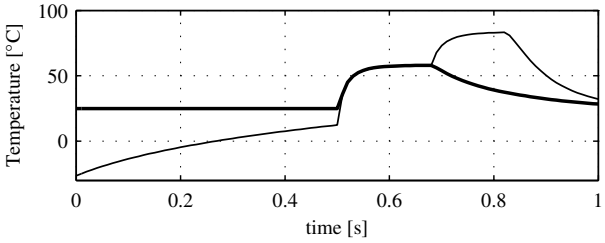



Fig. 8. Test 1: Module 2 temperature $T_2$ (bold line) and saturation temperature corresponding to the current pressure $P_2$ (thin line)

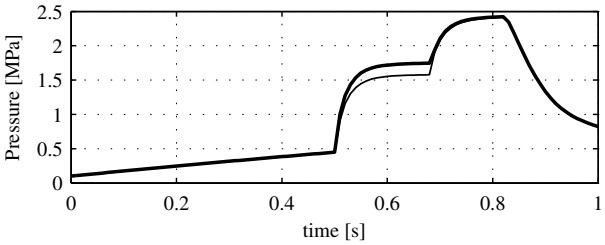



Fig. 9. Test 1: module pressures $P_1$ (bold line) and $P_2$ (thin line)

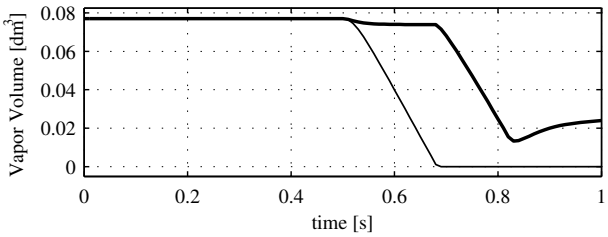



Fig. 10. Test 1: Module Vapor Volumes $V_{V1}$ (bold line) and $V_{V2}$ (thin line)

The results of the second test, namely Test 2, with large fluidic resistance between modules, i.e. $R_{fluid} = 3$MPa/(kg/s), are reported in Figs. 12–18. From Figs. 14 and 15, it can be noted that saturation phase takes place in Module 1 immediately after the input flow step, while in Module 2 this happens a little bit later, preceded by a period with negative vapor to liquid flow conversion ratio (see Fig.13). This is basically due to the large fluidic resistance between the two modules, preventing relevant mass flow (see Fig. 13). For the same reason subcooled phase occurs in Module 1, around $0.75$s in advance w.r.t Module 2, hence an opposite evolution takes place w.r.t. Test 1. With Module 1 in subcooled phase, the pressure $P_1$ shows a fast rising (see Fig. 16), again in accordance with lower equivalent capacity, then the mass flow from Module 1 to Module 2 increases and subcooled condition can take place also in Module 2 (at about $0.9$s), while Module 1 comes back to saturated phase.

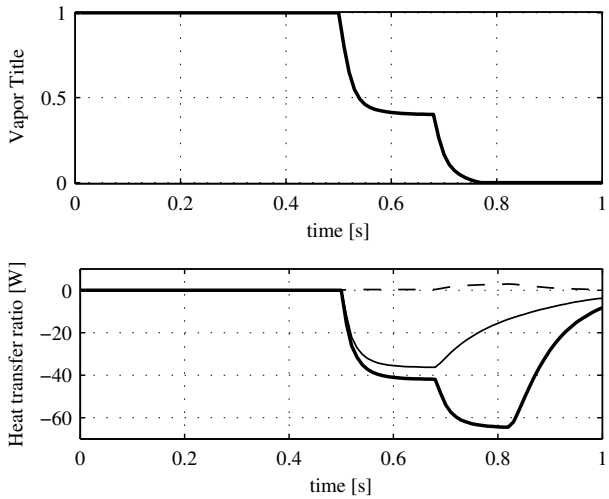



Fig. 11. Test 1: Vapor title at modules interface and heat transfer ratio at modules walls, $J_{QW1}$ (bold line), $J_{QW2}$ (thin line), and between modules (dashed)

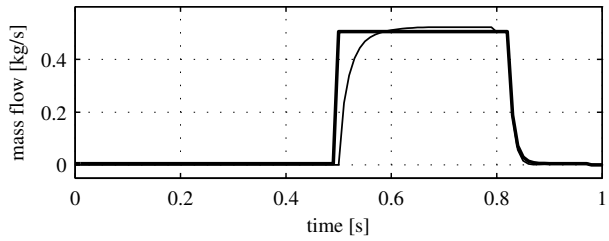



Fig. 12. Test 2: input vapor flow $\omega_{IV1}$ (bold line) and vapor-to-liquid exchange ratio in Module 1 $\omega_{V2L1}$ (thin line).

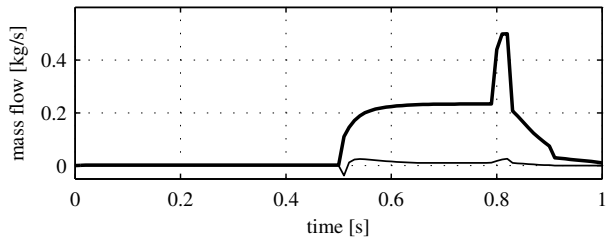



Fig. 13. Test 2: mass flow from Module 1 to Module 2 $\omega_{O1} = \omega_{I2}$ (bold line) and vapor-to-liquid exchange ratio in Module 2 $\omega_{V2L2}$ (thin line).

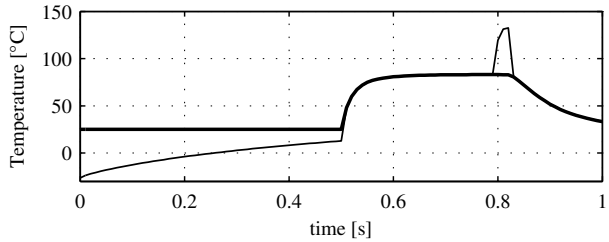



Fig. 14. Test 2: Module 1 temperature $T_1$ (bold line) and saturation temperature corresponding to the current pressure $P_1$ (thin line)

The proposed model, based on the composition of basic dynamic elements and exploiting a suitable vapor-to-liquid exchange rate computation in each element, shows the expected properties in constrained evolution representation. Hence, it is a promising step toward simple, but full representation of heat exchangers dynamics in VCC systems or other thermodynamic

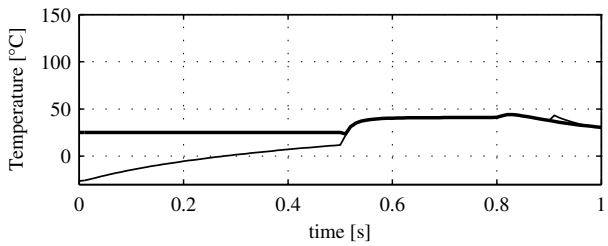



Fig. 15. Test 2: Module 2 temperature $T_2$ (bold line) and saturation temperature corresponding to the current pressure $P_2$ (thin line)

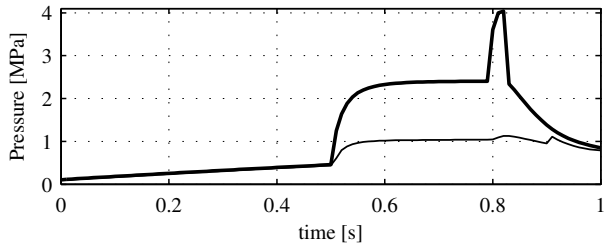



Fig. 16. Test 2: module pressures $P_1$ (bold line) and $P_2$ (thin line)

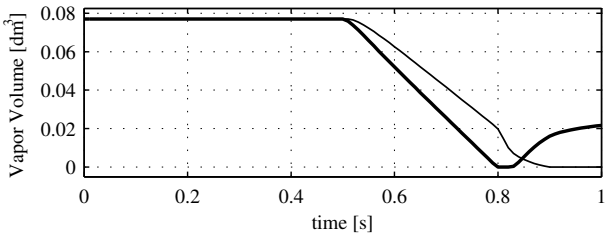



Fig. 17. Test 2: Module Vapor Volumes $V_{V1}$ (bold line) and $V_{V2}$ (thin line)

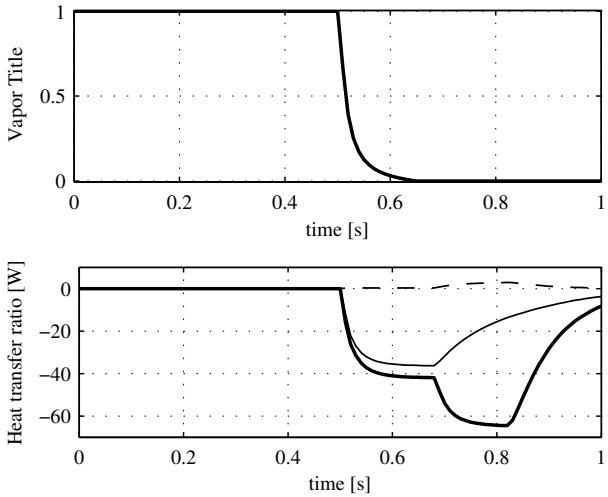



Fig. 18. Test 2: Vapor title at modules interface and heat transfer ratio at modules walls, $J_{Q_W 1}$ (bold line), $J_{Q_W 2}$ (thin line), and between modules (dashed)

cycles. Future efforts will be devoted to considering variable volume dynamic elements and to develop models for other components in VCC or general thermodynamic cycles, as compressors and valves. For the latter point, static model can be considered, according to compressor and valve fast dynamics w.r.t. heat exchangers, but the usual modelling solutions need to be carefully rearranged to define modules preserving the interface and the composability properties of the proposed approach.

## REFERENCES

A.G. Alleyne, B. Rasmussen, M. Keir and B. Eldredge. Advances in energy systems modeling and control. *Proc. of 2007 American Control Conference*, New York City, USA, pp.4363–4373, July 2007.

S. Bendapudi and J. E. Braun. A review of literature on dynamic models of vapor compression equipment. *ASHRAE Report*, Report #4036-5, 2002.

L. Bin and A. G. Alleyne. A full dynamic model of a HVAC vapor compression cycle interacting with a dynamic environment. *Proc. of 2009 American Control Conference*, St. Louis, MO, USA, pp.3662–3668, June 2009.

W.-D. Gruhle and R. Isermann. Modeling and control of a refrigerant evaporator. *Journal of Dynamic Systems, Measurement, and Control*, 107:235–240, 1985.

X.-D. He, S. Liu, and H. H. Asada. Modeling of vapor compression cycles for multivariable feedback control of HVAC systems. *Journal of Dynamic Systems, Measurement, and Control*, 119:183–191, 1997.

D. Leducq, J. Guilpart and G. Trystam. Low order dynamic model of a vapor compression cycle for process control design. *Journal of Food Process Engineering*, 26:67–91, 2003.

E. W. Lemmon, M. O. McLinden, and D. G. Friend. Thermophysical Properties of Fluid Systems. In P.J. Linstrom and W.G. Mallard (Eds.), *NIST Chemistry WebBook, NIST Standard Reference Database Number 69*, National Institute of Standards and Technology, Gaithersburg, MD, 20899, http://webbook.nist.gov, 2008.

J. W. MacArthur and E. W. Grald. Unsteady compressible two-phase flow model for predicting cyclic heat pump performance and a comparison with experimental data. *International Journal of Refrigeration*, 12:29–41, 1989.

T. L. McKinley and A. G. Alleyne. An advanced nonlinear switched heat exchanger model for vapor compression cycles using the moving-boundary method. *International Journal of Refrigeration*, 31:1253–1264, 2008.

N. B. O. L. Pettit, M. Willatzen and L. Ploug-Sørensen. A general dynamic simulation model for evaporators and condensers in refrigeration. Part II: simulation and control of an evaporator. *International Journal of Refrigeration*, 21:404–414, 1998.

C. K. Rice. The effect of void fraction correlation and heat flux assumption on refrigerant charge inventory predictions. *ASHRAE Transactions*, 93, Part 1:341–367, 1987.

A. Tilli and R. Diversi. Dynamical modelling of single–phase and two–phase states in thermodynamic cycles. *Preprints of the 8th IFAC Symposium on Nonlinear Control Systems*, Bologna, Italy, pp. 451–456, September 2010.

M. Willatzen, N. B. O. L. Pettit and L. Ploug-Sørensen. A general dynamic simulation model for evaporators and condensers in refrigeration. Part I: moving-boundary formulation of two-phase flows with heat exchange. *International Journal of Refrigeration*, 21:398–403, 1998.

W.-J. Zhang and C.-L. Zhang. A generalized moving–boundary model for transient simulation of dry–expansion evaporators under larger disturbances. *International Journal of Refrigeration*, 29:1119–1127, 2006.